Ciemat 693
Sp ISSN 614-087-X

CURRENT DRIVE BY ELECTRON CYCLOTRON WAVES IN STELLARATORS

por:

F. Castejón
C. Alejaldre
J. A. Coarasa

CENTRO DE INVESTIGACIONES

ENERGETICAS, MEDIOAMBIENTALES Y TECNOLOGICAS

MADRID,1992

CLASIFICACION DOE Y DESCRIPTORES

700350
MAGNETIC CONFINEMENT
ELECTRON CYCLOTRON-RESONANCE
NON-INDUCTIVE CURRENT DRIVE
PLASMA HEATING
STELLARATORS

Toda correspondencia en relación con este trabajo debe dirigirse al Servicio de Información y Documentación, Centro de Investigaciones Energéticas, Medioambientales y Tecnológicas, Ciudad Universitaria, 28040-MADRID, ESPAÑA.

Las solicitudes de ejemplares deben dirigirse a este mismo Servicio.

Los descriptores se han seleccionado del Thesauro del DOE para describir las materias que contiene este informe con vistas a su recuperación. La catalogación se ha hecho utilizando el documento DOE/TIC-4602 (Rev. 1) Descriptive Cataloguing On-Line, y la clasificación de acuerdo con el documento DOE/TIC.4584-R7 Subject Categories and Scope publicados por el Office of Scientific and Technical Information del Departamento de Energía de los Estados Unidos.

Este trabajo se ha recibido para su impresión en Febrero de 1.992.

Depósito Legal nº M-9487-1992
ISBN 84-7834-142-0
ISSN 614-087-X
NIPO 238-92-013-5

IMPRIME CIEMAT

I-INTRODUCTION

Current drive by microwaves in the range of the Electron Cyclotron Resonance frequency (EC-waves) has been experimentally demonstrated in tokamaks [1,2,3] and stellarators [4], with results that allow for a moderate optimism on the capability of this method to generate non-inductive currents in "next step" fusion devices. The motivation to use ECCD in Tokamaks is clear, microwaves in this frequency range can penetrate to the core of a reactor grade plasma and non-inductively drive current where it is needed. Stellarators, being "current-free" devices, do not need any such scheme to obtain particle confinement, all needed currents are produced by external coils. The usefulness of ECCD on stellarators, specially in shearless devices, lays on the possibility of using these waves to compensate intrinsic plasma currents like bootstrap that can be deleterious for confinement in the device. The clear experiments on Wendelstein VII-AS show how confinement is greatly improved when ECCD is used to compensate bootstrap and Pfirsch-Schlüter currents making the device a true current free stellarator [5]. This is particularly important in configurations, like the Heliac under construction in Madrid, TJ-II, with magnetic configurations having an iota -or q- profile practically shearless, where pressure driven currents can push the iota profile towards rational values with the corresponding consequences for confinement. Also, due to the extreme localization of EC waves power deposition, the possibility opens to use ECCD to locally control q-profiles [6], although this awaits experimental proof.

Current drive by EC-waves consists of the asymmetric modification of the electron resistivity in the momentum space [7]. Even a diffusion in the perpendicular momentum direction causes a net current, provided it is asymmetric in the parallel direction, by the modification of the collision frequency of the electrons. The resonant absorption modifies the distribution function which can be computed solving the Fokker-Planck equation (see e. g. [8, 9, 10]). Once the distribution function is known, the current density parallel to the magnetic field can be evaluated.

Such a calculation is expensive in terms of computational time. There are alternative methods which allow the estimation of the current without knowing the distribution function. Those methods are either based on the adjoint approach as presented in [11, 12], or on the Langevin equations [13], as the calculation

presented in this work. The last one gives the current drive efficiency for a test particle as:

$$\eta(\vec{p}) = \frac{\delta J_{\parallel}}{\delta P} = \frac{(\hat{s}\cdot\vec{\nabla})\chi(\vec{p})}{(\hat{s}\cdot\vec{\nabla})E(\vec{p})} \qquad (1),$$

where E is the kinetic energy of the resonant particle, the vector s is parallel to the diffusion direction in the momentum space, and is given by:

$$\vec{s} = \frac{s\omega_c}{\omega}\hat{e}_{\perp} + \left(\gamma - \frac{s\omega_c}{\omega}\right)\hat{e}_{\parallel} \qquad (2)$$

and χ is the so called response function, i. e., the total contribution of the particle to the current:

$$\chi(\vec{p}_0) = \int_0^{\infty} j_{\parallel}(t,\vec{p})dt = -e\int_0^{\infty} \frac{p_{\parallel}(t,\vec{p}_0)}{m\gamma}dt \qquad (3)$$

To calculate the response function one must know the test particle evolution in momentum space, that is obtained averaging Langevin equations for a particle ensemble embedded in a thermal bath [14].

This method gives a linear estimation of the induced current and is accurate if the absorbed power density is not very high and the distribution function not far from Maxwellian. The method is fast enough to allow the inclusion of the efficiency function in a ray tracing code, which calculates the absorbed power density and, therefore, the induced current in a complex magnetic configuration can be computed.

In the present work the induced current by EC waves is computed for the heliac TJ-II. The complex geometry of the machine is introduced in the ray tracing code RAYS [15] to calculate the absorbed power density profile. The width and structure of the microwave beam are taken into account since they are not negligible respect to the plasma size.

II-THE EFFICIENCY FUNCTION

The induced current density parallel to the magnetic field can be written in terms of the absorbed power density in phase space and the microscopic efficiency as follows :

$$J_{\parallel}(\vec{r}) = A\int d\vec{v}\frac{\delta J}{\delta P}\sum_{s} w_{s}(\vec{v}) \qquad (4)$$

The constant A is:

$$A = -\frac{mc^2}{8\pi n\,\Lambda\, e^3}$$

where n, m and e are the electron density, mass and charge, c is the speed of light and Λ is the Coulomb logarithm.

The efficiency can be obtained from the Langevin equations averaged for a Maxwellian distribution function in the high energy limit (see [13]). For the relativistic case and, in general, for oblique propagation, the efficiency is :

$$\eta(\vec{v}) = \frac{\delta J_{\parallel}}{\delta P_d} = G(v)\left[N_{\parallel} - \frac{v_{\parallel}}{v^2}(\gamma + 1 + Z)\right] + \frac{2vv_{\parallel}}{\gamma^2} \qquad (5),$$

where the function G(v) is given by:

$$G(v) = \frac{2}{v}\left[\frac{\gamma(v)+1}{\gamma(v)-1}\right]^{\frac{1+Z}{2}}\int_0^v dx\left[\frac{x}{\gamma(x)}\right]^3\left[\frac{\gamma(x)-1}{\gamma(x)+1}\right]^{\frac{1+Z}{2}} \qquad (6)$$

and we have adopted the following normalization:

$$\vec{v} = \frac{\vec{p}}{mc} \quad ; \quad \gamma = \left(1+v^2\right)^{1/2}$$

For Z_{eff}=1 the function G(v) can be computed analytically:

$$G(v) = 2\left(\frac{\gamma+1}{\gamma-1}\right)\frac{v^2 - 2\gamma\ln\gamma}{\gamma v} \qquad (7)$$

For arbitrary values of Z_{eff} the integral in (6) must be performed numerically. In figure 1 the efficiency is presented for some values of Z_{eff}. It is shown that the efficiency decreases with Z_{eff},

which means that the impurities have a negative influence on current drive efficiency and so do multiple charged ion plasmas. This is not surprising since the collision frequency rises with Z_{eff} and the particles are thermalized faster.

When varying the parallel refraction index, $N_{||}$, the efficiency rises for the momenta of the sign of the index, but falls in the opposite direction, as can be seen in figure 2. The efficiency is an odd function in $v_{||}$ when $N_{||}=0$ and is an even function in the product $v_{||}N_{||}$.

Rising the perpendicular momentum is in general deleterious for the efficiency, but for the values we consider here ($p_\perp/mc \approx 0.01$) it has no appreciable influence.

We consider the absorbed power density in phase space at harmonic s, w_s, which is different from zero only for the resonant electrons:

$$w_s(\vec{v}) \propto \delta\left(\gamma - \frac{s\omega_c}{\omega} - N_{||}v_{||}\right) \qquad (8)$$

This guarantees that we obtain zero current for $N_{||}=0$, since w_s is an even function and the efficiency an odd one. Moreover, as the efficiency is an even function in the product $v_{||}N_{||}$, changing the sign of $N_{||}$ will change the sign of the induced current density.

After integrating in $v_\perp$ in (4), the current density parallel to the magnetic field can be written as,

$$J_{||} = A\sum_{s=1}^{\infty}\int_{v_-}^{v_+} dv_{||}\,\eta(v_{||})\,w_s(v_{||}) \qquad (9)$$

The absorbed power density for a Maxwellian distribution function, at lowest order in Larmor radius, is given by (see e. g. [16]) :

$$w_s(v_{||}) = \frac{\mu^2\omega_p^2}{64\omega K_2(\mu)}\left(\frac{N_\perp\omega}{2\omega_c}\right)^{2(s-1)}\left(\frac{1}{(s-1)!}\right)^2 \times$$
$$\left|E_x - iE_y + \frac{N_\perp\omega}{s\omega_c}v_{||}E_z\right|^2 v_\perp^{2s}\exp(-\mu\gamma) \qquad (10)$$

In this linear theory, the efficiency has been calculated as an average in time and for a test ensemble of particles embedded in a Maxwellian distribution function, therefore it does not depend on the absorbed power density.

The result of making the integration for the O mode at first harmonic is shown in figure 3a, and for the X mode at second harmonic is shown in figure 3b. In both figures, the induced current is plotted versus frequency for several values of $N_{||}$, keeping constant the other plasma parameters. The absorbed power density is the same for all the cases in each plot. It can be seen that the current has opposite signs at upshifted and downshifted frequencies. The point where the current changes sign does not depend on $N_{||}$, but on the value of $Y_s=s\omega_c/\omega$. When $N_{||}$ is increased the induced current density becomes more unlocalized and falls. The difference between both figures, near the point where the current density is 0, can be explained considering the different expressions of the absorbed power density for X and O modes.

The deformation of the distribution function can be considered a perturbation of the Maxwellian, that we can assume that is well localized in the momentum space. The position of the deformation will be near the so called Collective Resonant Momentum [16]. This momentum is defined as the point in momentum space where the deformation in the distribution function is maximum or, equivalently, where absorbed power is maximum:

$$\frac{dw_s(v_{||})}{dv_{||}} = 0$$

This condition is fulfilled by these values of $v_{||}$:

$$v_{||R} \approx v_{R\pm} \equiv \frac{N_{||}Y_s}{1-N_{||}^2} + \frac{s}{\mu N_{||}} \pm \sqrt{\frac{N_{||}^2 - 1 + Y_s^2}{\left(1-N_{||}^2\right)^2} + \left(\frac{s}{\mu N_{||}}\right)^2} \qquad (11)$$

Only one of the two values is inside the resonant momentum interval, and it depends on the sign of $N_{||}$:

$$N_{||} < 0 \;\Rightarrow\; v_{||R} = v_{R+} \quad ; \quad N_{||} > 0 \;\Rightarrow\; v_{||R} = v_{R-}$$

The induced current density parallel to the magnetic field at a point in the plasma can be approximated by this expression [16, 17]:

$$j_{\parallel}(< r >) \approx A\eta(\vec{v}_R) < P_{cy} > \qquad (12)$$

where the efficiency is calculated at the Collective Resonant Momentum. This approximation can be avoided calculating numerically the momentum integral (9). In figure 4 the current density obtained by both methods at the second harmonic for X mode is shown. The Collective Resonant Momentum approximation (curve marked with squares) is accurate only at downshifted frequencies, but this estimation is not so good at upshifted frequencies and near the point where the current changes the its sign.

Moreover, the numerical integration allows the introduction of trapped particles effects, that are not evident using the Collective Resonant Moment approximation, because it gives null current when such momentum is in the trapping region.

III- INCLUSION OF TRAPPED PARTICLES

The effect of trapped particles on current drive can be important in stellarators, especially when ECRH is in consideration, since the diffusion in momentum space is mainly in the perpendicular direction and the stellarator configuration allows a big variety of trapping mechanisms.

As it is well-known, a particle with momentum v, whose guiding centre moves along a field line with momentum $v_{||}(t)$, is trapped if:

$$\frac{v_{||}}{v}(t) \le \mu_t \equiv \left(1-\frac{B}{B_{max}}\right)^{1/2} \qquad (13),$$

where μ_t is the trapping parameter, B is the local magnetic field and B_{max} is the maximum magnetic field on a field line. Since the field lines are dense on a magnetic surface, B_{max} coincides approximately with the maximum of the magnetic field at the magnetic surface. In a stellarator configuration, both fields must be calculated numerically using the Biot-Savart law [18].

Let us consider how trapped particles modify the efficiency (5). Trapped particles do not contribute to the current in the bounce average, so the efficiency is zero in the trapping region:

$$\eta_T(v_{||}) = 0 \quad ; \quad v_1 \le v_{||} \le v_2 \quad ,$$

$$v_{1,2} = \frac{Y_s N_{||} \mu_t^2 \pm \mu_t \left[Y_s^2 - 1 + \mu_t^2 N_{||}^2\right]}{1-\mu_t^2 N_{||}^2} \qquad (14)$$

Additionally, circulating particles can become trapped by the effect of the diffusion in momentum space and, from that moment on, they will not contribute to the current, which must be taken into account in the calculation. The contribution of this kind of particles modifies the response function as follows [19]:

$$\chi_T(\vec{v}) = \chi(\vec{v}) - \frac{v_{||}}{|v_{||}|}\chi(\vec{v}_T) \qquad (15).$$

v_T is the momentum when the particle starting with momentum v becomes trapped. That momentum is calculated using the Langevin equations, averaged over an ensemble of particles. The

results we have obtained for its parallel component and module are:

$$(v_T)_{\parallel} = \frac{v_{\parallel}}{|v_{\parallel}|}\mu_t v_T \qquad \text{and} \qquad v_T = \frac{2\sqrt{g(\vec{v})}}{1-g(\vec{v})} \tag{16},$$

where we have introduced the function:

$$g(\vec{v}) = \left(\frac{\mu_t v}{|v_{\parallel}|}\right)^{\frac{2}{Z+1}} \frac{\gamma-1}{\gamma+1} \tag{17}.$$

Using equation (1) we obtain the efficiency in presence of trapped particles, outside the trapping region:

$$\eta_T(\vec{v}) = \eta(\vec{v}) - \frac{v_{\parallel}}{|v_{\parallel}|}\frac{1+2g(\vec{v})}{(1-g(\vec{v}))^2\sqrt{g(\vec{v})}}\left(\frac{\mu_t v}{|v_{\parallel}|}\right)^{\frac{2}{Z+1}} \frac{\partial\chi(\vec{v}_T)}{\partial v_T}\left(\frac{\gamma-1}{\gamma+1}\right)\frac{1}{v^2} \times$$

$$\times\left\{2+\frac{2}{Z+1}\left[Y_s - v_{\parallel}N_{\parallel}\left(\frac{v_{\perp}}{v_{\parallel}}\right)^2\right]\right\} \tag{18},$$

where the derivative of the response function is given by:

$$\frac{\partial\chi(v_T)}{\partial v_T} = \mu_t\left[2\left(\frac{v_T}{\gamma_T}\right)^3 - (Z+1)\frac{1}{\gamma_T}G(v_T)\right] \tag{19}$$

and $\eta(v)$ is the efficiency without trapped particles, given by equation (5). The sign of $\eta_T(v)$ can be opposite to the sign of $\eta(v)$.

Then, we evaluate the integral (9) introducing the efficiency (18) and obtain the induced current density in presence of trapped particles. In figure 5a the influence of trapped particles on EC current drive efficiency is shown. The induced current density parallel to the magnetic field is plotted versus frequency for X mode at second harmonic and different values of the trapping parameter. The nature of EC diffusion in momentum space, which is mainly in the perpendicular direction, makes the effect of trapped particles deleterious, and the module of the induced current density falls when μ_t rises. Even a change in the current direction is possible when trapping parameter is large enough.

The effect of trapped particles changes with $N_{||}$. This is because the number of resonant electrons which are trapped varies and their contribution to the current also varies. This can be understood considering the expression inside the integral of (9): When $N_{||}$ rises, the resonance curve in momentum space moves in the positive direction of $v_{||}$ and the maximum of the expression inside the integral goes into the trapping region and then goes out. The induced current versus frequency, for different values of $N_{||}$, is plotted in figure 6, we have taken a medium value for the trapping parameter μ_t=0.2. It is shown that, when $N_{||}$ rises, the peak of positive current which appears at upshifted frequencies moves to the right and its maximum is not monotonous.

IV - ADAPTATION TO A RAY TRACING CODE

To take into account refraction effects and the complex magnetic geometry of stellarators, we included the expression (9), with the efficiency (18), in the ray tracing code RAYS [20]. The parameters needed to calculate the efficiency are given by the code. We assume that the resonant electrons move on the magnetic surfaces and are quickly mixed with the rest. The current is then uniform on each magnetic surface and we calculate the averaged absorbed power density inside a given magnetic surface [21], considering the differential volume of the whole magnetic surface.

The induced current at a point in the plasma can be written in terms of the absorbed power density, at the considered harmonic s, as:

$$J_{\parallel}(\vec{r}) = \gamma(\vec{r}) W_s(\vec{r}) \qquad (20),$$

where the global current drive efficiency has been introduced:

$$\gamma(\vec{r}) = \frac{A \int d\vec{v}\, \eta_T(\vec{v}) \sum_s w_s(\vec{v})}{\int d\vec{v} \sum_s w_s(\vec{v})} \qquad (21)$$

$W_s(r)$, the averaged absorbed power density at a magnetic surface, is calculated as follows:

$$W_s(\vec{r}) = \frac{\Delta P(\vec{r})}{2\pi^2 R_0 \left(2\rho(\vec{r})\delta + \delta^2\right)} \qquad (22)$$

We have defined:

$$\rho(\vec{r}) = \begin{cases} < r >, |\vec{r}| > b \\ b, |\vec{r}| \le b \end{cases} \qquad (23)$$

and

$$\delta = \max\left\{ \Delta < r >, b \sin\left(\frac{\vec{k} \cdot \vec{\nabla}\Psi}{|\vec{k}||\vec{\nabla}\Psi|} \right) \right\} \qquad (24)$$

ΔP is the power absorbed in a ray step, given by the code, R_0 is the major radius, $\langle r \rangle$ is the mean minor radius of the magnetic surface, b is the width of a single ray, **k** is the wave vector, Ψ is the toroidal flux and $\Delta\langle r \rangle$ is the variation of the mean radius in the ray step, calculated from flux coordinates. The parameter δ is chosen to take into account the fact that when the ray is not nearly perpendicular to the magnetic surface (the direction given by the flux gradient) only a fraction of the power carried by the ray is deposited at such surface.

To obtain the toroidal component of the current density one must perform:

$$J_\phi(\vec{r}) = J_\parallel(\vec{r}) \frac{B_\phi(\vec{r})}{B(\vec{r})} \qquad (25),$$

where $B_{\vec{\phi}}$ is the toroidal component of the magnetic field and B its module.

From this expression, one sees that the averaged power density can be raised when the ray path is almost parallel to the surface. It is also possible that a ray crosses twice the same magnetic surface. In the last case the induced current density depends on the local plasma parameters of the crossing points and the total current density at the surface is obtained adding all the single surface cross contributions. In this way we obtain an expression for the current density induced by one ray, which is function of the magnetic surface, i. e., of the mean minor radius.

The microwave beam structure must be taken into account, because its width in TJ-II is d=5 cm, which is not negligible respect to the plasma dimensions. We take a squared Gaussian beam simulated by a number L^2 of rays and we disregard the four corner rays. The width of a single ray is b=d/L. This will make the absorption area more unlocalized in the plasma than when only one ray is considered [17], so the current profiles we obtain are wider. Additionally, the several ray paths can be very different and so do the plasma characteristics where the absorption happens, namely the values of the density, temperature, parallel index and magnetic field. Hence, the absorbed power and the induced current densities are different for the several rays of the beam. The averaged absorbed power density, which depends on the angle between the wave vector and the toroidal flux gradient, can change, especially when the ray beam diverges.

The total toroidal current density at each magnetic surface is obtained adding the currents induced by every ray:

$$J_\phi(<r>) = \frac{1}{\sum_{i=rays} \exp\left(-x_i^2/(d/2)^2\right)} \sum_{i=rays} J_\phi(<r>,i) \exp\left(-x_i^2/(d/2)^2\right) \tag{26}$$

In the same way, the global absorbed power density can be calculated:

$$W_s(<r>) = \frac{1}{\sum_{i=rays} \exp\left(-x_i^2/(d/2)^2\right)} \sum_{i=rays} W_s(<r>,i) \exp\left(-x_i^2/(d/2)^2\right) \tag{27}$$

The current intensity is calculated in terms of the mean radii of the magnetic surfaces. To perform the integration it is necessary to consider the current perpendicular to the toroidal surface, i. e. :

$$I = \int \vec{J} \cdot d\vec{S} = 2\pi \int_0^a <r> J_\phi(<r>)\, d<r> \tag{28}$$

The amount of induced current depends on many factors, which vary from a ray to another. The fraction of absorbed power at downshifted or upshifted frequencies changes, which modifies the sign of the current density. Generally speaking, a good efficiency will be obtained when one has strong well-localized absorption because it happens only at upshifted frequencies, for low field side injection, or downshifted frequencies, from high field side injection.

The influence of trapped particles depends on the chosen position for the injection. The role played by them is more important when absorption happens at external magnetic surfaces. This is because the maximum magnetic field on a magnetic surface rises for increasing mean minor radius. The toroidal positions of the beam for which the plasma is far from the device axis present also important trapped particle effects, since the local field is lower. In some cases trapped particle effects can even change the sign of the current.

V - NUMERICAL APPLICATION TO TJ-II

The TJ-II heliac [22, 23] is a medium size, ℓ=1, M=4 stellarator under construction in Madrid. Its minor radius can vary depending on the magnetic configuration between a=0.1-0.20 m, its mean major radius is R_0=1.5 m, the magnetic field in the centre of the plasma is about 1 T. Its magnetic configuration is characterized mainly by having a helical magnetic axis and beam shaped magnetic surfaces. The microwave injection will be done by two 200 kW gyrotrons which emit at 53.2 GHz, i. e., at the second harmonic frequency. For the present work we choose a configuration with a=0.17 m.

The total amount of induced current is calculated simulating the microwave beam by 144 rays (L=12) and disregarding the four corner rays. As the beam is 5 cm wide, the distance between the rays will be b=0.4166 cm, narrow enough to simulate a continuum. The difference between the mean radii of contiguous magnetic surfaces is taken to be 0.5 cm, which is a good approximation, taking into account the transversal separation of the rays. The induced current is calculated by linear interpolation in the mean minor radius.

The cases presented here correspond to the toroidal position of 16.8º for only one gyrotron. The geometrical position for the injection and the TJ-II plasma are shown in figure 7. The effect of both gyrotrons can be obtained by adding the density currents induced by each one. The azimutal and poloidal angles of injection, φ and θ, can be varied to study the behaviour of the induced current. By varying these angles one can change the amount and the sign of the current and the current density profile. The electron density on axis is n_0=1.5 x 10^{19} m^{-3} and the electron temperature on axis is T_0=0.8 keV, which are typical values we expect to reach in TJ-II. The toroidal magnetic field is in the negative direction, i. e., in the clockwise direction.

The control over the induced current is not absolute because one must consider other important effects. First of all we have refraction. When one changes the injection angles of the beam, the angle between the normal to magnetic surfaces and the wave vector is changed, so refraction effects can deviate the beam. Second, the absorbed power density in plasma depends on the value of $N_{||}$, therefore the fraction of absorbed power at downshifted or upshifted frequencies along one ray path changes when varying $N_{||}$, which changes the sign of the induced current density, as it has been shown in section II. The width of the

microwave beam is also a limitation in order to control the induced current, since the absorption area is quite wide and one can have some rays which induce a current in one direction and others in the opposite one. Trapped particles may have an important influence because when the absorption happens in magnetic surfaces far from the axis, their effect can be very important.

The average power density, and hence, the amount of induced current density, are higher near the magnetic axis, since the volume of heated plasma is smaller, so the amount of current one can get off axis is smaller.

First, we present the case of absorption on axis, so that absorbed power density is quite high. The position of the antenna is chosen just in the vertical below the magnetic axis, 35 cm under the equatorial plane, as it is shown in figure 7. We choose $\varphi=106.8^{o}$ and vary θ. The ray paths are presented for $\theta=15^{o}$ in figure 8, where only 9 rays are plotted for clarity. In figure 9 the profiles of absorbed power and the toroidal component of the induced current densities, averaged to the magnetic surface, are plotted for this case. One can see that the current is pretty high and well localized in this case, since the absorption is strong, on axis and at downshifted frequencies. The total current will be I=-1.68 kA. Even though the angle is positive, $N_{||}$ is negative because the field is in the negative toroidal direction, and varies between $N_{||}=-0.05$ and $N_{||}=-0.15$ for the different rays in the resonant region.

In figure 10 we present a case in which $\theta=-5^{o}$. We see that power absorption occurs near the axis and for positive $N_{||}$, so we obtain a positive current of I=2.58 kA.

In the third case, which is presented in figure 11, the amount of induced current is small because $N_{||}$ is small and we have current density of both signs, positive and negative. This has been obtained for $\theta=7.5^{o}$. The absorbed power density and the toroidal induced current density are high near the magnetic axis because the volume and the surface in which they are calculated are small. The power absorption profile is quite wide due to refraction effects. Even though the microwaves are almost perpendicular to the magnetic field, the ray paths are not normal to the surfaces of constant refractive index, therefore those effects are important in this case. The width of the radial grid has been taken of 0.8 cm in this case in order to mask the discrete beam structure.

In figure 12 we present the induced current intensity and the global absorbed power for different values of the angle θ. We see that the change of the sign does not occur at $\theta=0^o$ but at about $\theta=7.5^o$, because the effects of refraction. These effects make the absorption fall for oblique injection and, therefore, the amount of induced current also falls.

We consider now situations in which the absorption happens off-axis. These are obtained for $\theta=15^o$, when the ray paths are outside the vertical direction, and different values of φ. Varying this angle we can change the sign and the amount of the current as is shown in figures 13 and 14. In figure 13 we have taken $\varphi=216^o$ and obtained a positive current of about 0.32 kA; the power deposition profile is wide and pretty flat. On the other hand, in figure 14, the current is negative and higher: I=-1.4 kA and the absorbed power density is similar to the former case; this is obtained for $\varphi=187^o$.

Trapped particle effects are important near the edge where the trapping parameter is high and where the temperature is still high enough to maintain a low collisional regime. We consider two situations in which the absorption occurs near the edge, but still for quite high temperature, in order that the collisions are not important as a detrapping cause. In this case the trapped particles play an important role and can reduce the current in an important amount. In figure 15a the injection angles are $\theta=25^o$ and $\varphi=187^o$ and the induced current in presence of trapped particles (I=-0.66 kA) is reduced to almost one half of the calculated disregarding their effect (I=-1.1 kA). In figure 15b, for $\theta=35^o$ and $\varphi=187^o$, the amount of induced current is reduced from I=-0.38 kA, disregarding trapped particles, to I=-0.12 kA, including trapped particle effects.

V- CONCLUSIONS

In shearless stellarators even low currents (a few kA typically) can modify their confinement properties. The current induced by radio frequency can be useful to compensate deleterious currents like bootstrap or to modify the iota profile. The EC-waves can be appropriate for this goals, provided the relative control over the current density profile and over the amount of current one can achieve by varying the injection parameters.

The current density has been computed in this work from the efficiency in the momentum space and from the absorbed power density in phase space. The first one is obtained from Langevin equations averaged for a test ensemble of particles embedded in a thermal bath. The results obtained in this way are compared with those obtained by the Collective Resonant Momentum approximation and it is shown that such an approximation is only accurate at downshifted frequencies.

The influence of trapped particles is considered too. It is important especially in stellarators for two reasons: a) the diffusion caused by EC-waves is mainly in the perpendicular direction in momentum space and b) the fraction of resonant trapped particles depends on the toroidal and poloidal angles of the microwave injection and on the geometry of the device.

To estimate in an accurate way the induced current in a stellarator it must be taken into account the actual geometry of the device. In this work, this has been done using a ray tracing code. The volume of every magnetic surface and its section have been calculated using flux coordinates. Moreover, for medium side devices the microwave beam structure cannot be neglected, since its wide is comparable to the plasma size. This will cause the absorption be unlocalized and the current profile be wider, which impose limitations to the induced current control.

VII- ACKNOWLEDGEMENTS

The authors would like to thank Dr. V. Krivenski for his useful suggestions and discussions.

REFERENCES

[1] H. TANAKA, A. ANDO, K. OGURA, S. IDE, M. IIDA, K. OHO, S. OZAKI, K. IWAMURA, A. YAMAZAKI, M. NAKAMURA, T. MAEKAWA, Y. TERUMICHI, S. TANAKA, "Electron-Cyclotron Current Drive at the Second Harmonic in the WT-3 Tokamak," Physical Review Letters **60**, 1033 (1988).

[2] V.-V. ALIKAEV, "Electron Cyclotron Current Drive Experiments in the T-10 Tokamak," Bulletin of the American Physical Society **36**, 2296 (1991).

[3] R.-J. JAMES, G. GIRUZZI, A. FYARETDINOV, B. DE GENTILE, YU. GORELOV, R. HARVEY, S. JANZ, J. LOHR, T.-C. LUCE, K. MATSUDA, P. POLITZER, R. PRATER, L. RODRIGUEZ, R. SNIDER, V. TRUKHIN, "Electron Cyclotron Current Drive Experiments on DIII-D," Proceedings of the 17th European Conference on Controlled Fusion and Plasma Physics. EPS, part III, 1259, Amsterdam (1990).

[4] H. RENNER, W7AS TEAM, NBI GROUP, ICF GROUP, ECRH GROUP, "Initial operation of the Wendelstein 7AS advanced stellarator," Plasma Physics and Controlled Fusion **31**, 1579 (1989) .

[5] U. GASPARINO, V. ERCKMANN, H. MAABBERG, W7AS TEAM, "Non-inductive currents in W VII-AS," Proceedings of the 17th European Conference on Controlled Fusion and Plasma Physics. EPS, part III, 1275, Amsterdam (1990).

[6] F. CASTEJON, A.-L. FRAGUAS, A. VARIAS, "Stabilization of local modes by Electron Cyclotron Current Drive," Bulletin of the American Physical Society **36**, 2343 (1991).

[7] N.-J. FISCH, A.-H. BOOZER, "Creating an asymmetric plasma resistivity with waves," Physical Review Letters **45**, 720 (1980).

[8] C.-F.-F. KARNEY, N.-J. FISCH, "Numerical studies of current generation by radio-frequency travelling waves," Physics of Fluids **22**, 1817 (1979).

[9] D.-F.-H. START, M.-R. O'BRIEN, P.-V.-M. GRACE, "The effect of a relativistic resonance condition on the Fokker-

Planck theory of ECRH Current Drive," Plasma Physics **25**, 1431 (1983).

[10] I. FIDONE, G. GIRUZZI, V. KRIVENSKI, E. MAZZUCATO, L.-F. ZIEBELL, "Cross effects on Electron Cyclotron and Lower Hybrid Current Drive in tokamak plasmas," Nuclear Fusion **27**, 579 (1987).

[11] S.-P. HIRSHMAN, "Classical collisional theory of beam-driven plasma currents," Physics of Fluids **23**, 1238 (1980).

[12] V. ERCKMANN, U. GASPARINO, H. MAABBERG, H. RENNER, M. TUTTER, W7AS TEAM, "Electron Cyclotron Current Drive and wave absorption experiments in the W 7-AS stellarator," IAEA-CN-53/ C-3-1 (1990).

[13] N.-J. FISCH, "Current generation in a relativistic plasma," Physical Review A **24**, 3245 (1980)

[14] D. MOSHER, "Interactions of relativistic electron beams with high atomic number plasmas," Physics of Fluids **18**, 846 (1974)

[15] R. C. GOLDFINGER, D. B. BATCHELOR, "Theory of Electron Cyclotron Heating in the ATF torsatron," Nuclear Fusion **27**, 31 (1987).

[16] I. FIDONE, G. GRANATA, J. JOHNER, "Current sustainment by synchrotron radiation in tokamaks," Physics of Fluids **31**, 2300 (1988)

[17] F. CASTEJON, C. ALEJALDRE, "Linear evaluation of current drive in TJ-II," Proceedings of the 17th European Conference on Controlled Fusion and Plasma Physics. EPS, part III, 1255, Amsterdam (1990).

[18] V.-E. LYNCH, B.-A. CARRERAS, L.-A. CHARLTON, L. GARCIA, T.-C. HENDER, H.-R. HICKS , J.-A. HOLMES, "Stellarator expansion methods for MHD Equilibrium and Stability calculations," Journal of Computational Physics **66**, 411 (1986).

[19] G. GIRUZZI, "Impact of electron trapping on RF current drive in tokamaks," Nuclear Fusion **27**, 1933 (1987)

[20] C. ALEJALDRE, F. CASTEJON, M. J. TABOADA, "Ray tracing with non-Maxwellian distribution functions. A case example: Heliac TJ-II", Proceedings of the 16th European Conference on Controlled Fusion and Plasma Physics. EPS, part III, 1115 Venice (1989).

[21] V. KRIVENSKI, I. FIDONE, G. GIRUZZI, G. GRANATA, R.-L. MEYER, E. MAZZUCCATO, "Improving current generation in a tokamak by Electron Cyclotron waves," Nuclear Fusion **25**, 127 (1985) .

[22] T.-C. HENDER, J.-L. CANTRELL, J.-H. HARRIS, B.-A. CARRERAS, V.-E. LYNCH, J.-F. LYON, J.-A. FABREGAS, J. GUASP, A. LOPEZ-FRAGUAS, A. P. NAVARRO, "Studies of a Flexible Heliac Configuration," Fusion Technology **13**, 515 (1988).

[23] C. ALEJALDRE, J. ALONSO, J. BOTIJA, F. CASTEJON, J. CEPERO, J. GUASP, A.-L. FRAGUAS, L. GARCIA, V. KRIVENSKI, R. MARTIN, A.-P. NAVARRO, A. PEREA, A. RODRIGUEZ-YUNTA, M. SOROLLA, A. VARIAS, "TJ-II Project: A Flexible Heliac Stellarator," Fusion Technology **17**, 131 (1990).

FIGURE CAPTIONS

Figure 1.- Current drive efficiency in momentum space versus parallel momentum for some values of Z_{eff}. We have taken $N_{||}=0.2$ and $v_{\perp}=0.1$. One sees that when Z_{eff} rises the absolute value of induced current falls.

Figure 2.- Current drive efficiency in momentum space versus parallel momentum for some values of $N_{||}$. We have taken $Z_{eff}=1$ and $v_{\perp}=0.1$. It can be seen that for $N_{||}=0$ the efficiency is an odd function.

Figure 3a.- Induced current density for different values of $N_{||}$ versus frequency for O mode at first harmonic. We have taken the following plasma parameters: Magnetic field B=1 T (f_c=28 GHz), electron density n=0.5 x 10^{19} m^{-3}, electron temperature T=1 keV and $Z_{eff}=1$. One sees that for rising $N_{||}$ the induced current density is lower and more unlocalized.

Figure 3b.- Induced current density for different values of $N_{||}$ versus frequency for X mode at second harmonic. We have taken the following plasma parameters: Magnetic field B=1 T ($2f_c$=56 GHz), electronic density n=1 x 10^{19} m^{-3}, electron temperature T=1 keV and $Z_{eff}=1$. One sees that for rising $N_{||}$ the induced current density is lower and more unlocalized, as in the former case.

Figure 4.- Comparison of induced current calculated by numerical integration and by using the Collective Resonant Momentum approximation. We have considered the same plasma parameters as in figure 3b and $N_{||}=0.2$.

Figure 5.- Induced current density by X mode microwaves, in presence of trapped particles for different values of trapping parameter μ_t and for frequencies near second harmonic. We have taken the same plasma parameters as in figure 4. For rising trapping parameter the absolute value of the current density falls, and in some cases a change of sign is possible .

Figure 6.- Induced current density, for the same plasma parameters as in figure 5, versus frequency. In this case the value of $N_{||}$ has been varied in order to study the effect of trapped particles for different angles of microwave propagation. The trapping parameter considered is $\mu_t=0.2$.

Figure 7.- TJ-II plasma rounding the circular central coil. Microwave beam situation is also plotted, the toroidal angle, $\phi=16.8^{o}$, is fixed for all the cases and so are the coordinates Z=-35

cm and R=152.5 cm. To obtain different currents we vary the angles φ and θ.

Figure 8.- Plot of ray paths, magnetic surfaces (dashed lines) and lines of |B|=constant for $\varphi=106.8^{o}$ and $\theta=15^{o}$. Only 9 rays have been plotted for clarity. The plasma region where absorption happens is marked by crosses and, as can be seen, is quite broad for this wide beam. The plasma parameter we have considered are: electron density on magnetic axis $n_0=1.5 \times 10^{19}$ m^{-3}, electron temperature on axis $T_0=0.8$ keV, $Z_{eff}=1$, magnetic field on axis $B_0=0.95$ T. The microwave frequency is 53.2 GHz and the injected power is 200 kw.

Figure 9.- Induced toroidal current density profile (continuous line) and absorbed power density profile (dashed line) versus mean minor radius in TJ-II, for the same plasma parameters and injection position as in figure 8.

Figure 10.- The same as in figure 9, for the same value of φ and for $\theta=-5^{o}$.

Figure 11.- The same as in figures 9 and 10, for the same value of φ and for $\theta=7.5^{o}$.

Figure 12.- Induced current (continuous line) and absorbed power (dashed line) for the same value of φ and for different values of θ. The cases calculated are marked in the plot. The plasma parameter are the same as in former four figures.

Figure 13.- Induced toroidal current density profile (continuous line) and absorbed power density profile (dashed line) versus mean minor radius in TJ-II, for the same plasma parameters but for injection angles $\varphi=215.8^{o}$ and $\theta=15^{o}$.

Figure 14.- The same as in figure 13, for the same value of θ and for $\varphi=186.8^{o}$.

Figure 15a.- Study of trapped particles effects. Absorbed power density (dashed line) and induced toroidal current density (continuous lines) versus mean minor radius for $\theta=25^{o}$ and for $\varphi=186.8^{o}$. The curve J1 is calculated taking into account trapped particles and the curve J2 is calculated disregarding these effects.

Figure 15b.- The same as in figure 15a, for the same value of φ and for $\theta=35^{o}$. The trapped particle effects are stronger in this case because the absorption happens at outer plasma positions and, hence, the trapping parameter is higher.

Figure 1

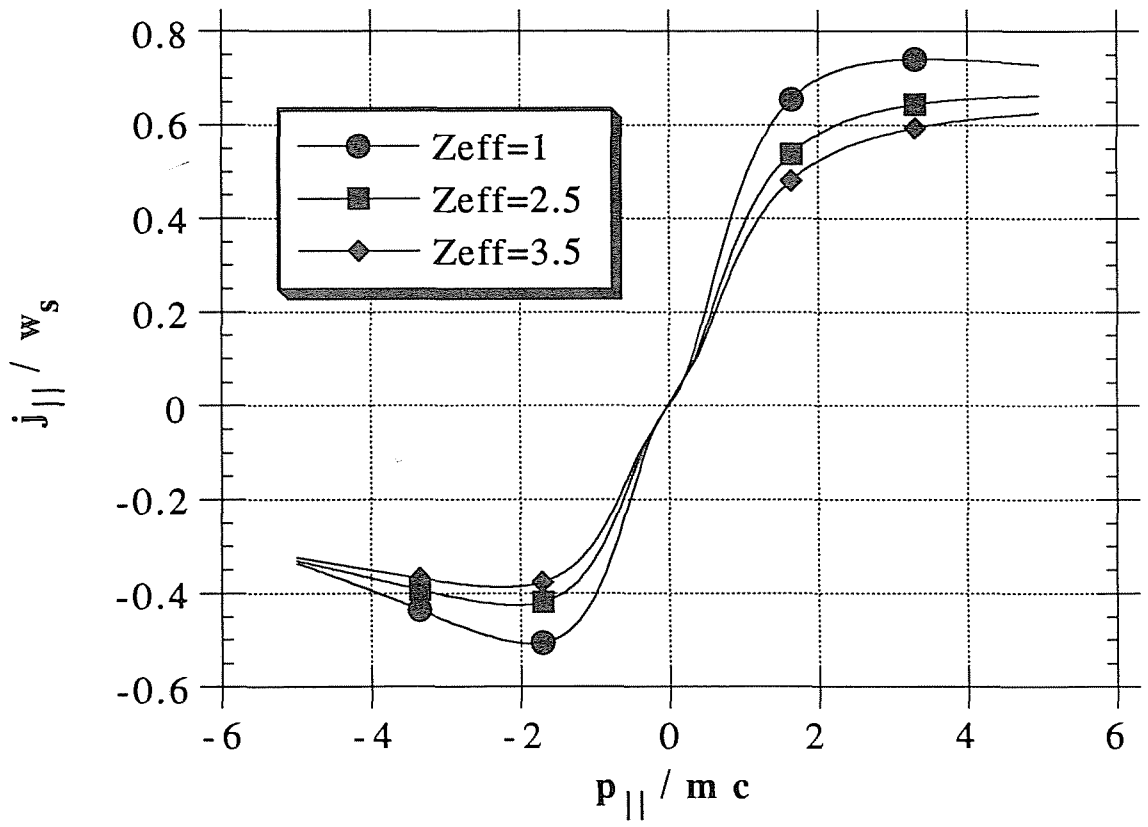

Figure 2

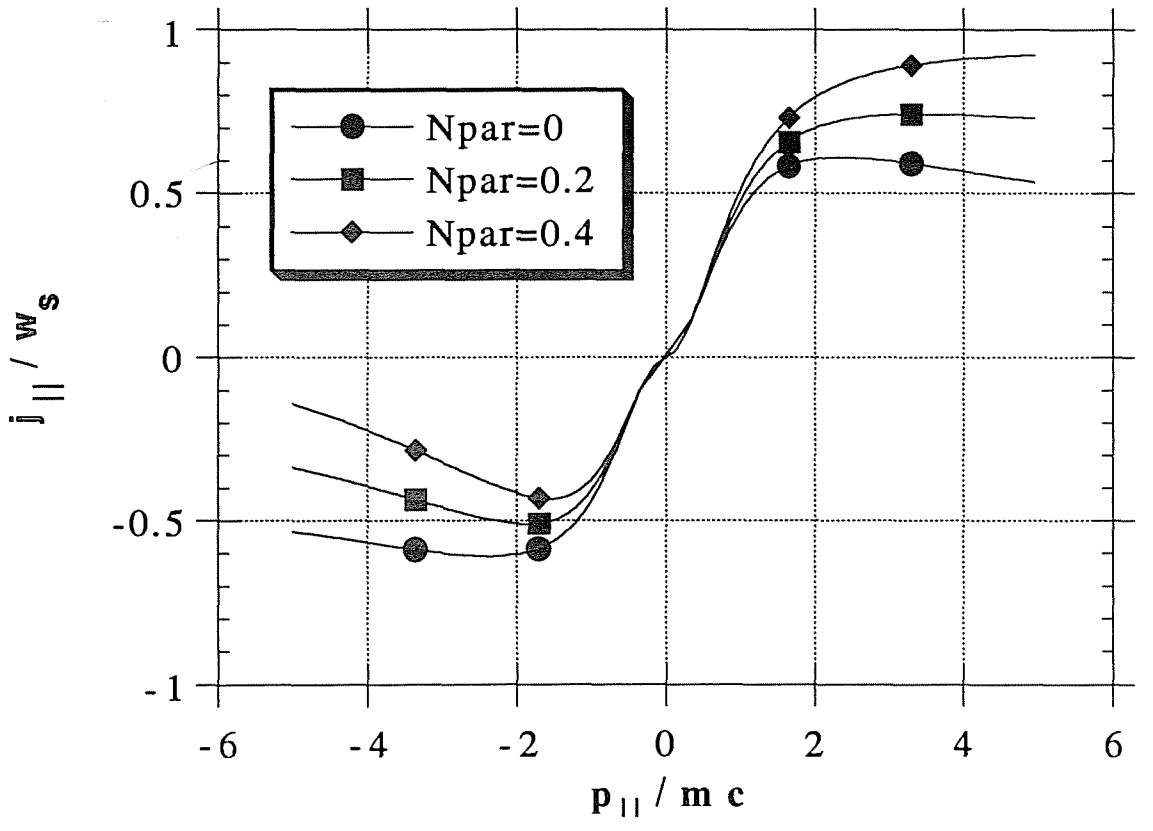

Figure 3a

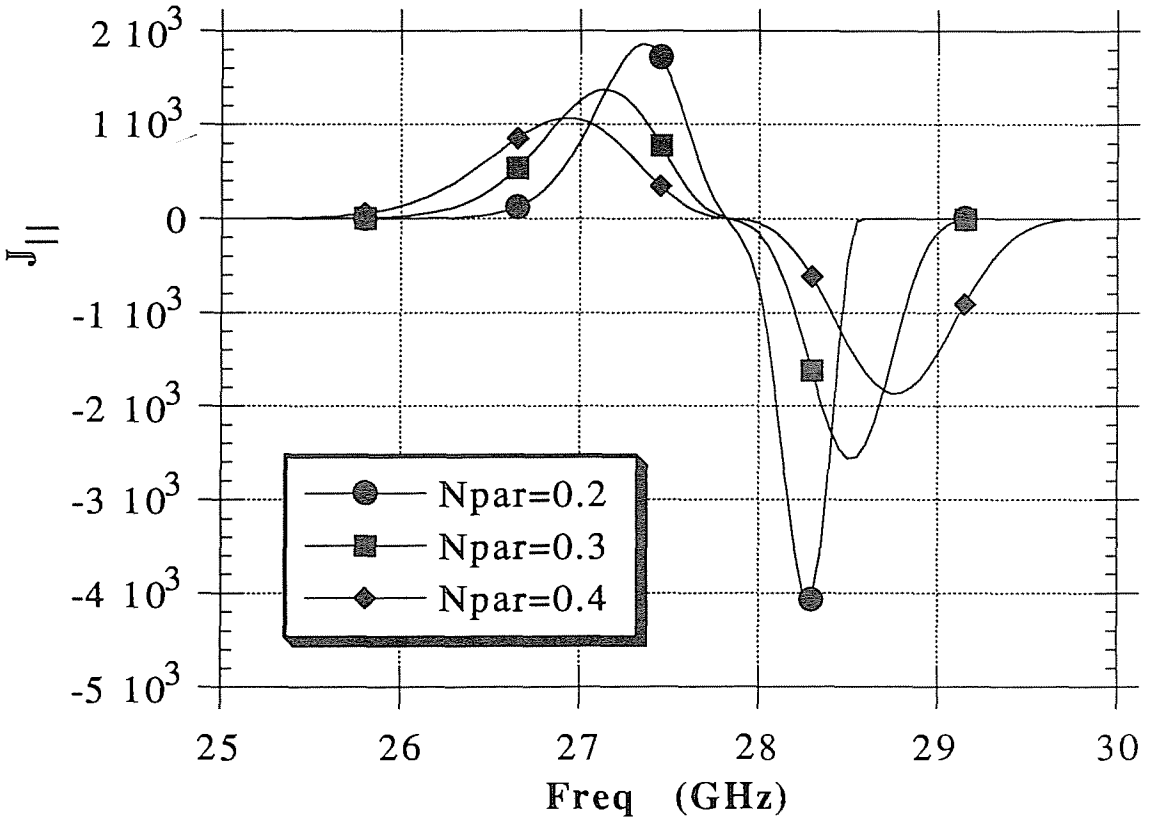
2 10^3
1 10^3
0
-1 10^3
-2 10^3
-3 10^3
-4 10^3
-5 10^3
J11
25
26
27
28
29
30
Freq (GHz)
Npar=0.2
Npar=0.3
Npar=0.4

Figure 3b

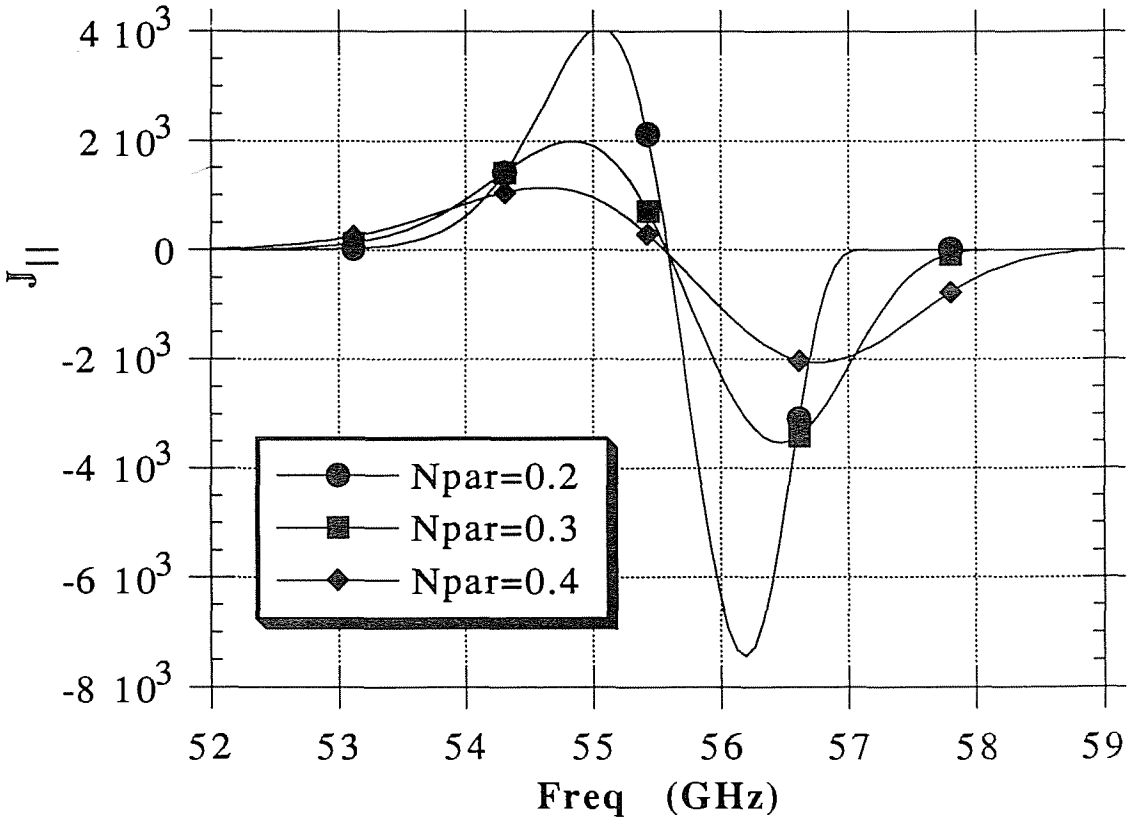
4 10^3
2 10^3
0
-2 10^3
-4 10^3
-6 10^3
-8 10^3
J||
52
53
54
55
56
57
58
59
Freq (GHz)
Npar=0.2
Npar=0.3
Npar=0.4

Figure 4

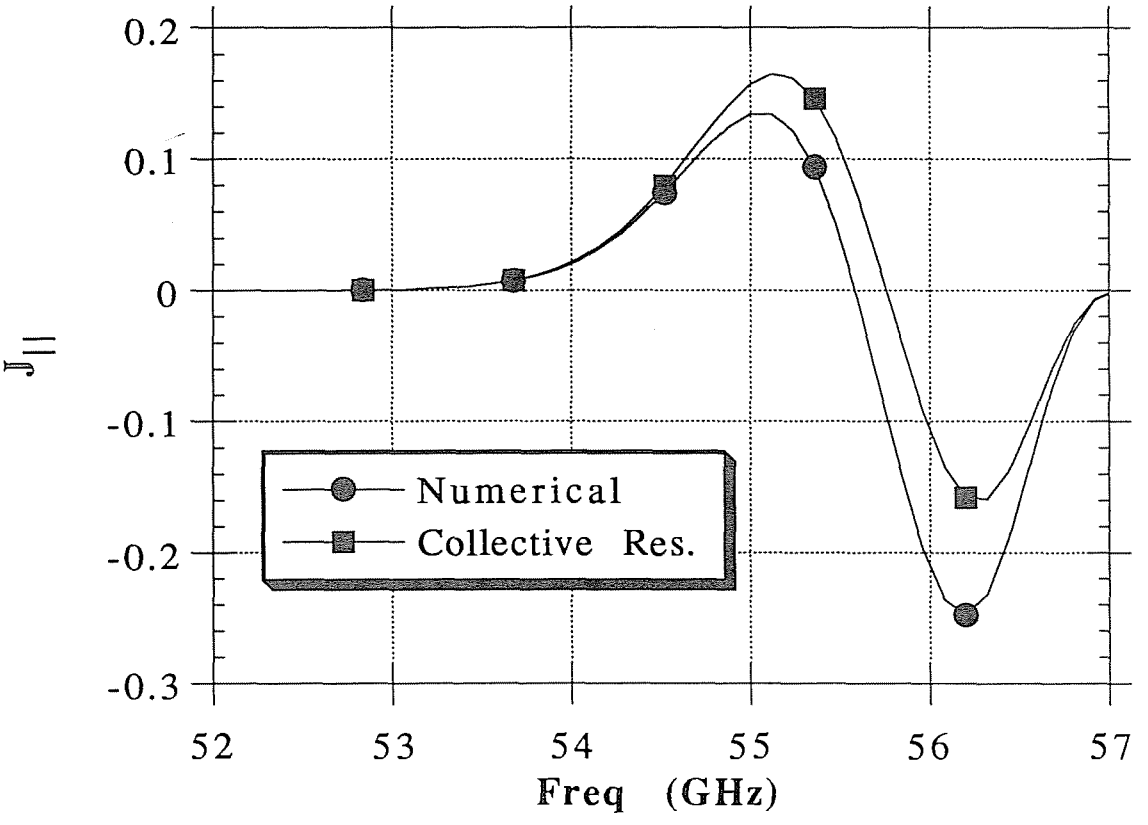
0.2
0.1
0
-0.1
-0.2
-0.3
J_{11}
Numerical
Collective Res.
52
53
54
55
56
57
Freq (GHz)

Figure 5

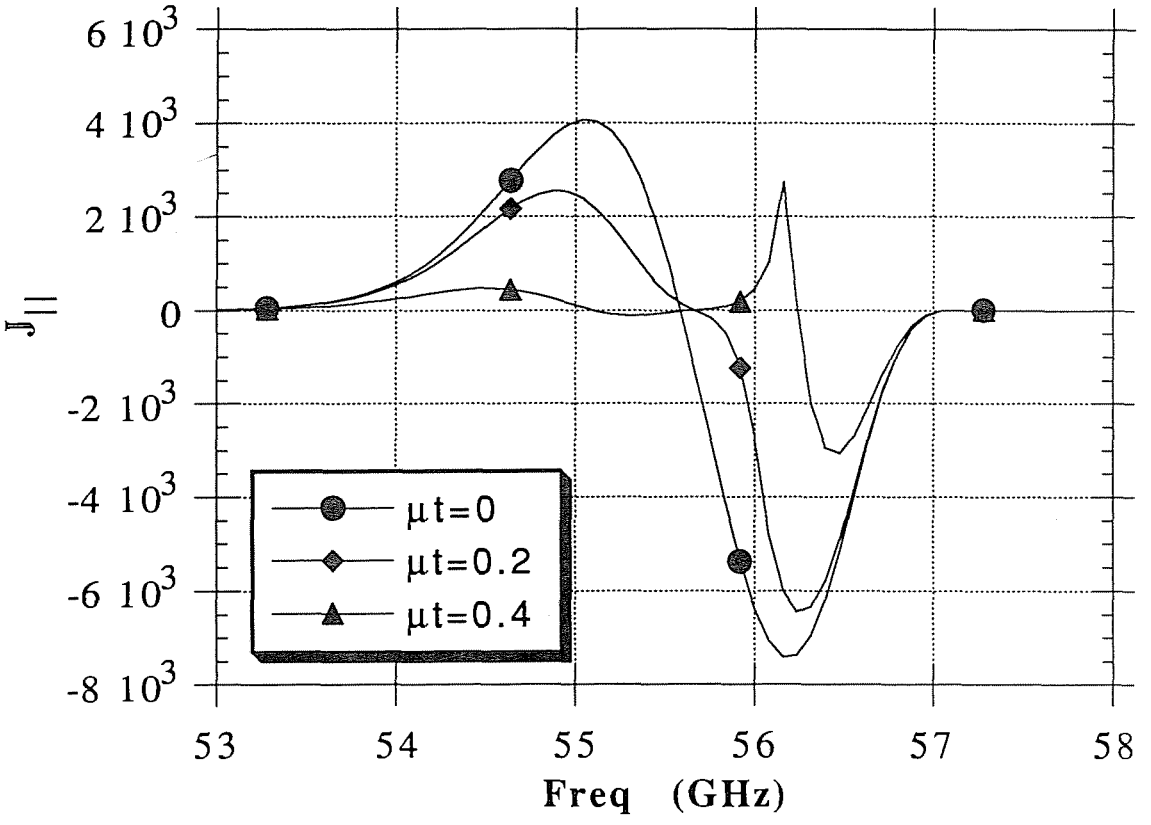
6 10^3
4 10^3
2 10^3
0
-2 10^3
-4 10^3
-6 10^3
-8 10^3
53
54
55
56
57
58
Freq (GHz)
μt=0
μt=0.2
μt=0.4

Figure 6

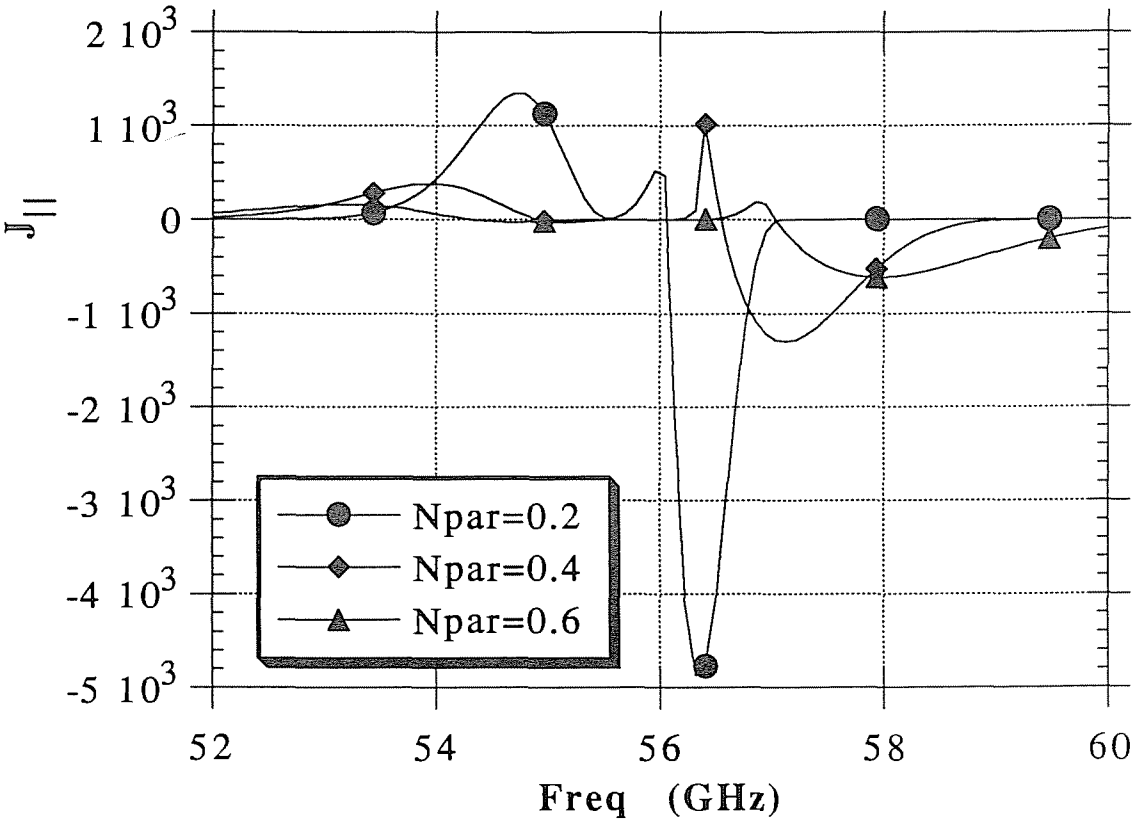
2 10^3
1 10^3
0
-1 10^3
-2 10^3
-3 10^3
-4 10^3
-5 10^3
52
54
56
58
60
Freq (GHz)
Npar=0.2
Npar=0.4
Npar=0.6

Figure 7

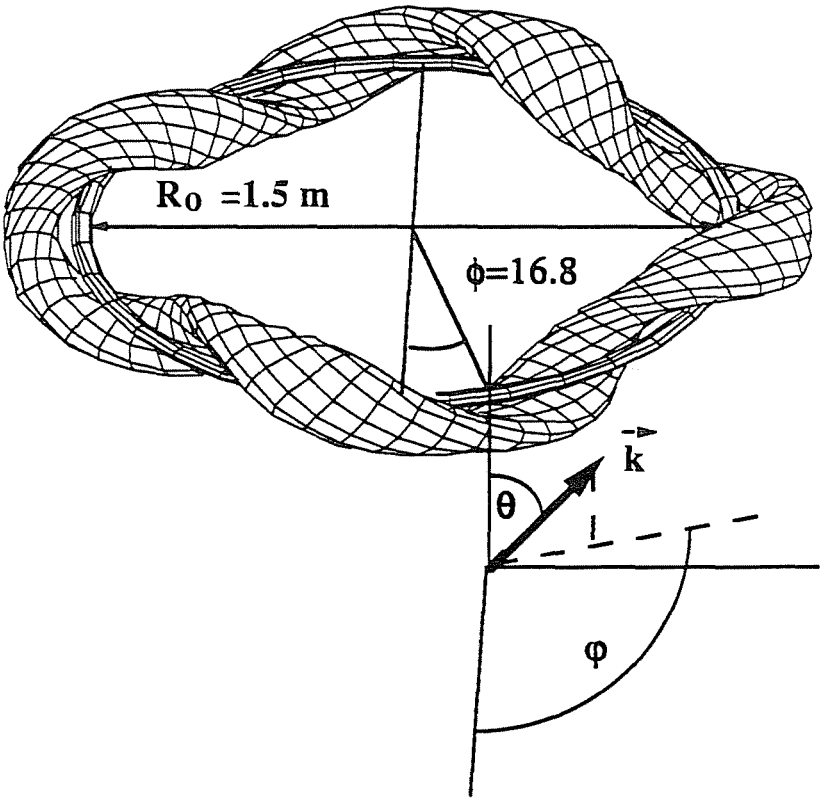

Figure 8

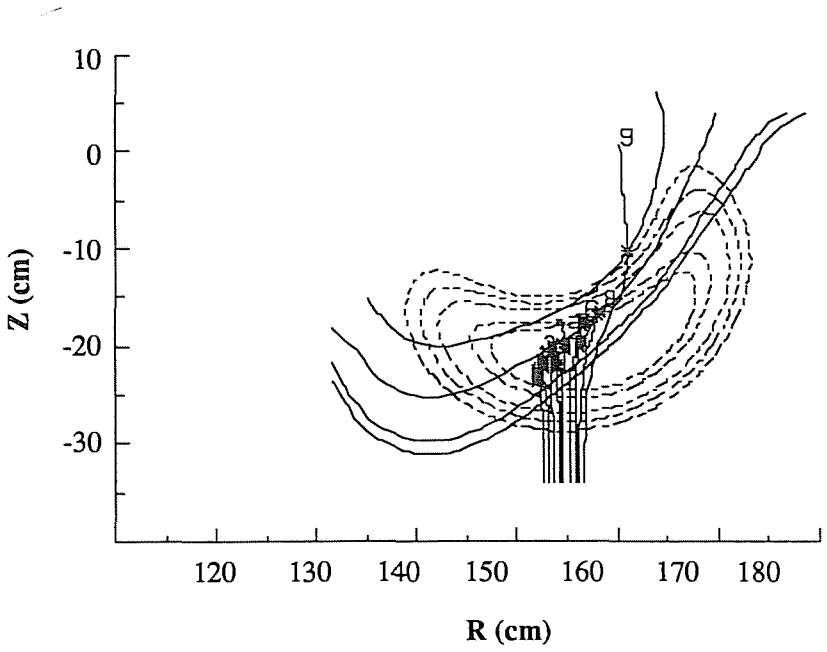

Figure 9

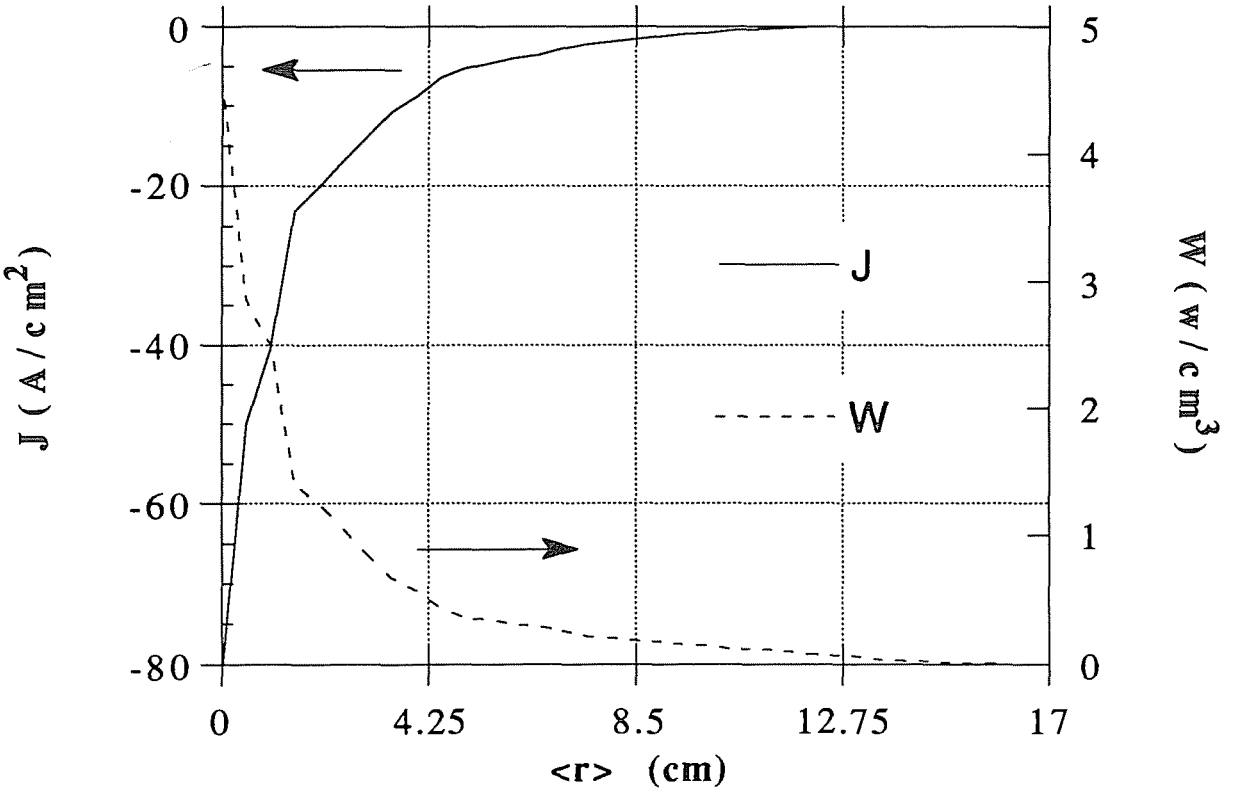

Figure 10

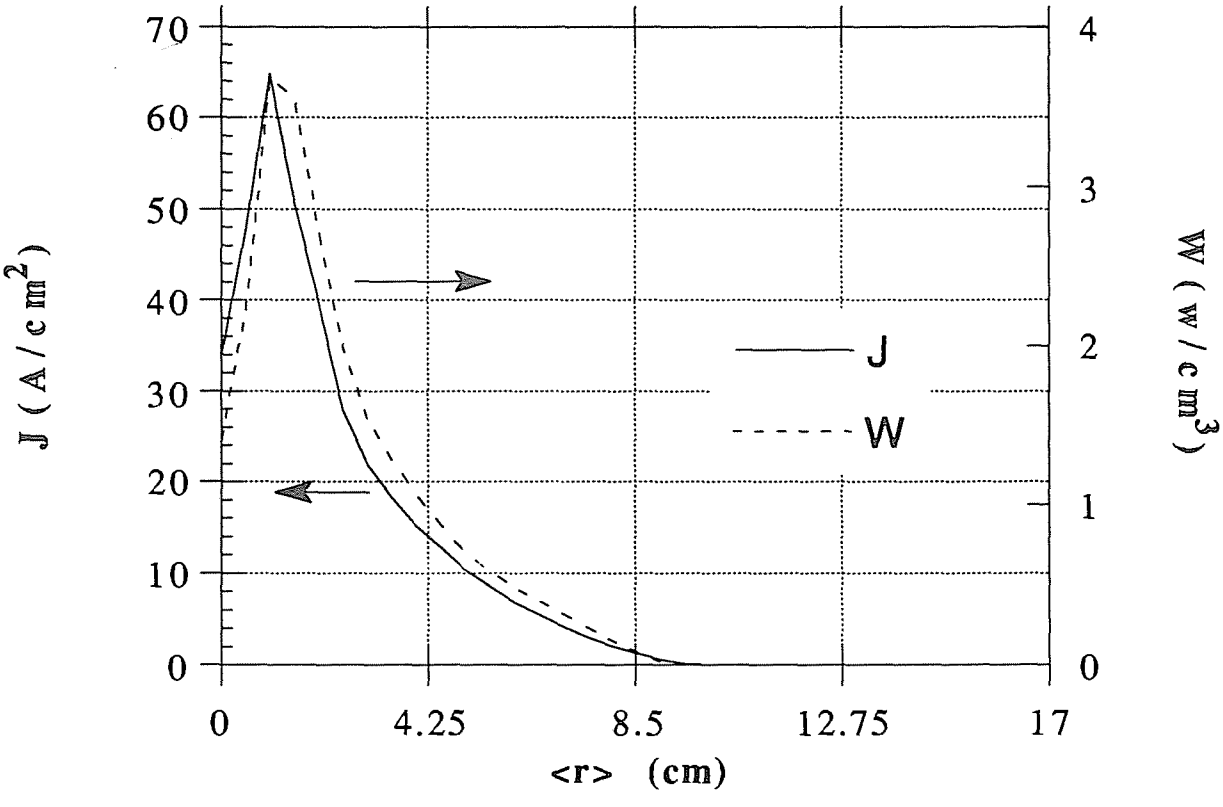

Figure 11

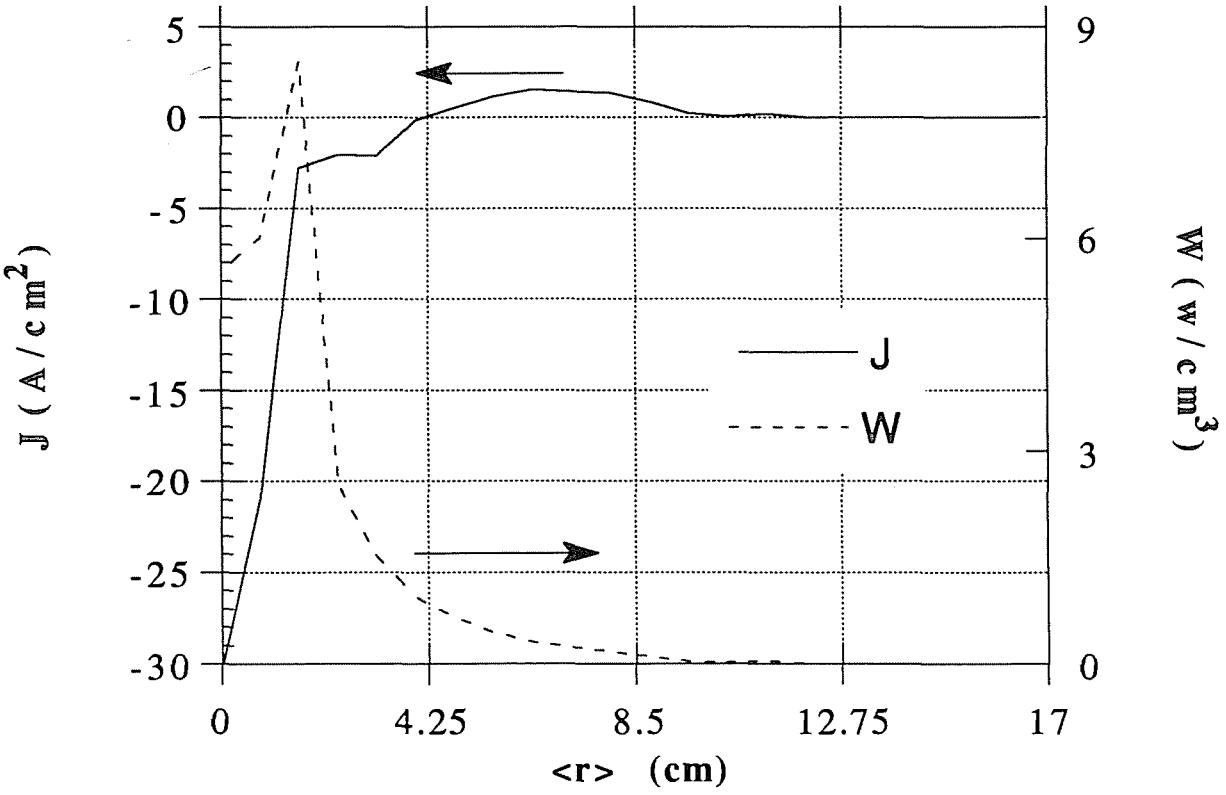

Figure 12

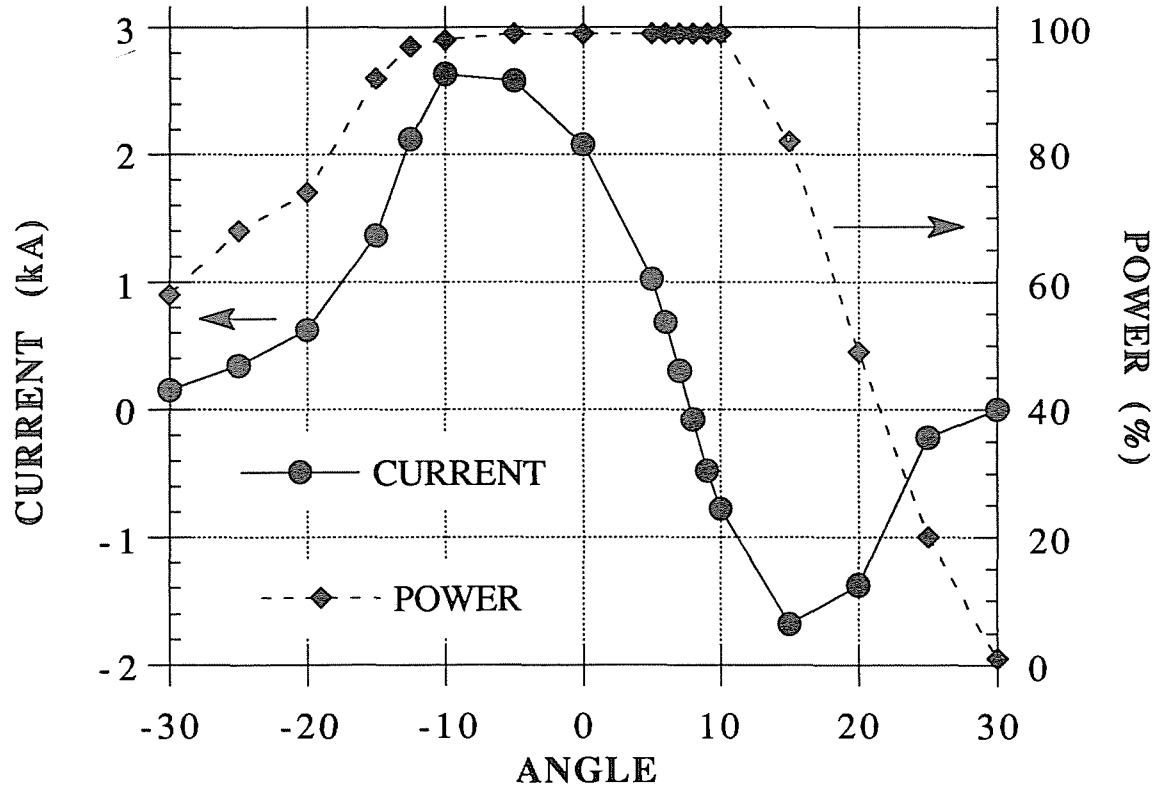
CURRENT (kA)
POWER (%)
ANGLE
CURRENT
POWER
3
2
1
0
-1
-2
100
80
60
40
20
0
-30
-20
-10
0
10
20
30

Figure 13

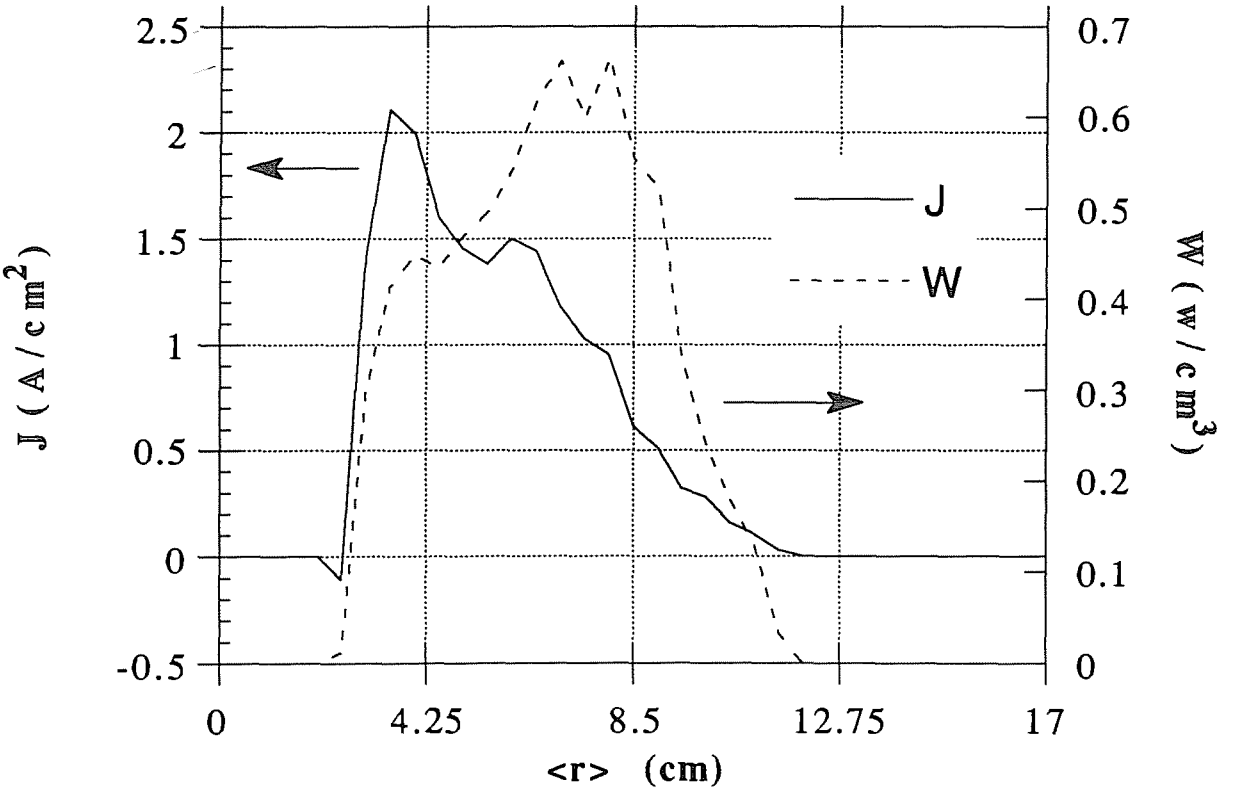
2.5
2
1.5
1
0.5
0
-0.5
J (A / c m^2)
0.7
0.6
0.5
0.4
0.3
0.2
0.1
0
W (w / c m^3)
J
W
0
4.25
8.5
12.75
17
<r> (cm)

Figure 14

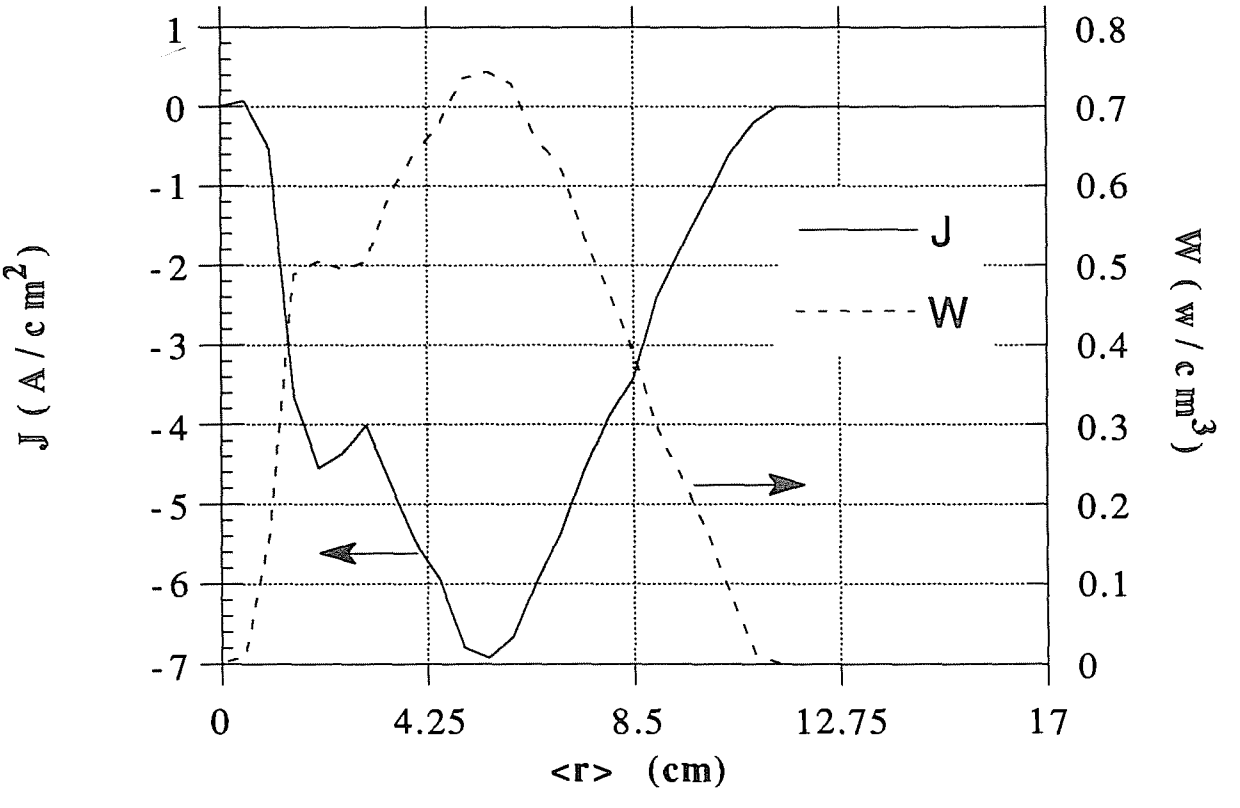
1
0
-1
-2
-3
-4
-5
-6
-7
J (A / c m^2)
0.8
0.7
0.6
0.5
0.4
0.3
0.2
0.1
0
W (w / c m^3)
J
W
0
4.25
8.5
12.75
17
<r> (cm)

Figure 15a

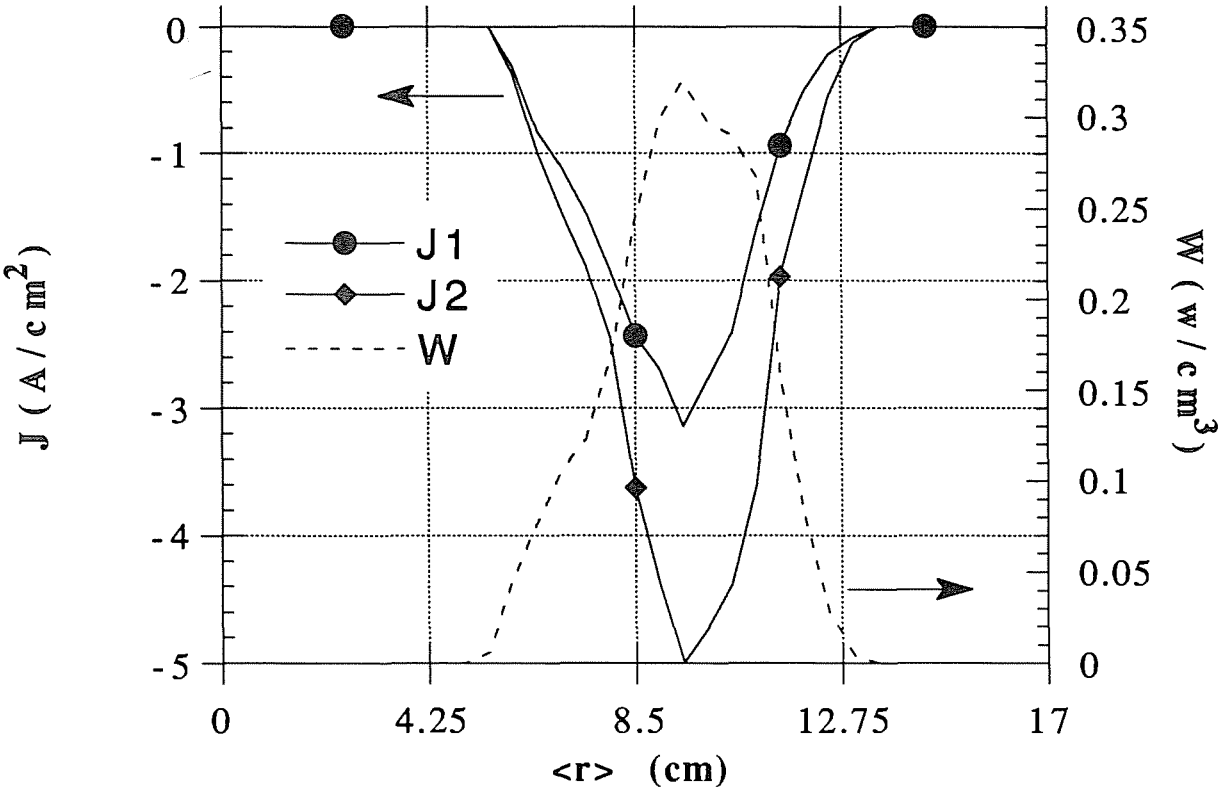
0
-1
-2
-3
-4
-5
0.35
0.3
0.25
0.2
0.15
0.1
0.05
0
J1
J2
W
J (A / c m^2)
W (w / c m^3)
0
4.25
8.5
12.75
17
<r> (cm)

Figure 15b

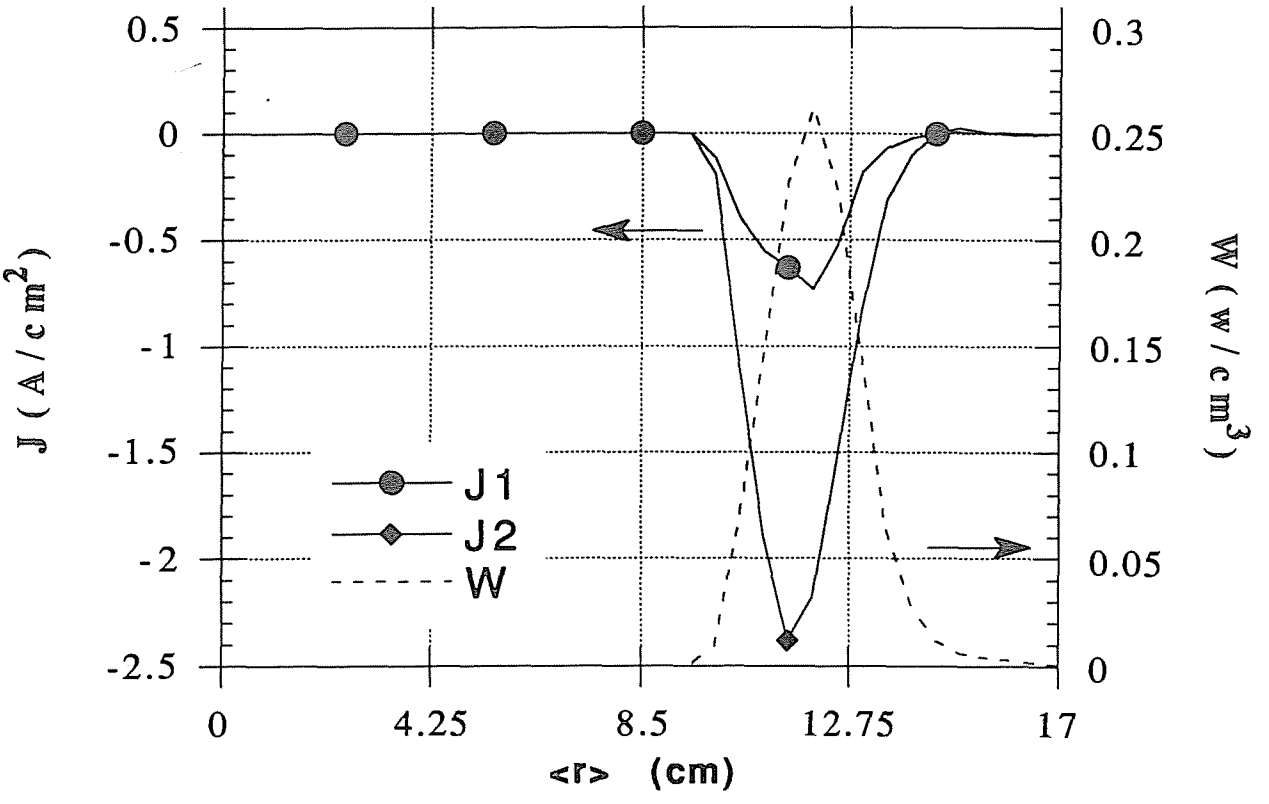
0.5
0
-0.5
-1
-1.5
-2
-2.5
0.3
0.25
0.2
0.15
0.1
0.05
0
0
4.25
8.5
12.75
17
J (A / c m^2)
W (w / c m^3)
<r> (cm)
J1
J2
W

CIEMAT-693

Centro de Investigaciones Energéticas, Medioambientales y Tecnológicas
Instituto de Investigación Básica.- MADRID

"Corriente contínua por ondas electrón-ciclotrón en estellaratores".

CASTEJON, F.; ALEJALDRE, C.; COARASA, J.A. (1992) 38 pp., 17 figs., 23 refs.

En este trabajo proponemos un método para calcular la corriente inducida por las microondas, en el rango de la frecuencia ciclotrónica electrónica, lo bastante rápido para ser incluído en un trazado de rayos y de esta forma tener en cuenta la complicada geometría de los estellaratores.Los efectos de las partículas atrapadas son particularmente importante en este método de inducción de corrientes en estellaratores, por lo tanto son tenidos en cuenta mediante la modificación que introducen en la eficiencia de la inducción de corrientes.

Básicamente el método consiste en integrar en el espacio de momentos el producto de la eficiencia relativista, corregida con los efectos de las partículas atrapadas, por la densidad de potencia absorbida en el espacio de fases. Esta última se calcula para una distribución Maxwelliana, ya que se supone que estamos en un régimen aproximadamente lineal. La influencia de las impurezas y de tener plasmas de otras especies que no sean protones se considera calculando la eficiencia para $Z_{eff} \neq 1$.

Finalmente se ha realizado un análisis numérico particularizado al Heliac Flexible TJ-II. La densidad de potencia absorbida se calcula mediante el trazado de rayos RAYS, teniendo en cuenta la estructura real del haz de microondas, cuya anchura no es despreciable frente al tamaño del plasma.

CLASIFICACION DOE Y DESCRIPTORES: 700350. Magnetic Confinement. Electrón Cyclotron-Resonance. Non-Inductive Current Drive. Plasma Heating. Stellarators.

CIEMAT-693

Centro de Investigaciones Energéticas, Medioambientales y Tecnológicas.
Instituto de Investigación Básica.- MADRID.

"Corriente contínua por ondas electrón-ciclotrón en estellaratores".

CASTEJON, F.; ALEJALDRE, C.; COARASA, J.A. (1992) 38 pp., 17 figs., 23 refs.

En este trabajo proponemos un método para calcular la corriente inducida por las microondas, en el rango de la frecuencia ciclotrónica electrónica, lo bastante rápido para ser incluído en un trazado de rayos y de esta forma tener en cuenta la complicada geometría de los estellaratores.Los efectos de las partículas atrapadas son particularmente importante en este método de inducción de corrientes en estellaratores, por lo tanto son tenidos en cuenta mediante la modificación que introducen en la eficiencia de la inducción de corrientes.

Básicamente el método consiste en integrar en el espacio de momentos el producto de la eficiencia relativista, corregida con los efectos de las partículas atrapadas, por la densidad de potencia absorbida en el espacio de fases. Esta última se calcula para una distribución Maxwelliana, ya que se supone que estamos en un régimen aproximadamente lineal. La influencia de las impurezas y de tener plasmas de otras especies que no sean protones se considera calculando la eficiencia para $Z_{eff} \neq 1$.

Finalmente se ha realizado un análisis numérico particularizado al Heliac Flexible TJ-II. La densidad de potencia absorbida se calcula mediante el trazado de rayos RAYS, teniendo en cuenta la estructura real del haz de microondas, cuya anchura no es despreciable frente al tamaño del plasma.

CLASIFICACION DOE Y DESCRIPTORES: 700350. Magnetic Confinement. Electrón Cyclotron-Resonance. Non-Inductive Current Drive. Plasma Heating. Stellarators.

CIEMAT-693

Centro de Investigaciones Energéticas, Medioambientales y Tecnológicas.
Instituto de Investigación Básica.- MADRID.

"Corriente contínua por ondas electrón-ciclotrón en estellaratores".

CASTEJON, F.; ALEJALDRE, C.; COARASA, J.A. (1992) 38 pp., 17 figs., 23 refs.

En este trabajo proponemos un método para calcular la corriente inducida por las microondas, en el rango de la frecuencia ciclotrónica electrónica, lo bastante rápido para ser incluído en un trazado de rayos y de esta forma tener en cuenta la complicada geometría de los estellaratores.Los efectos de las partículas atrapadas son particularmente importante en este método de inducción de corrientes en estellaratores, por lo tanto son tenidos en cuenta mediante la modificación que introducen en la eficiencia de la inducción de corrientes.

Básicamente el método consiste en integrar en el espacio de momentos el producto de la eficiencia relativista, corregida con los efectos de las partículas atrapadas, por la densidad de potencia absorbida en el espacio de fases. Esta última se calcula para una distribución Maxwelliana, ya que se supone que estamos en un régimen aproximadamente lineal. La influencia de las impurezas y de tener plasmas de otras especies que no sean protones se considera calculando la eficiencia para $Z_{eff} \neq 1$.

Finalmente se ha realizado un análisis numérico particularizado al Heliac Flexible TJ-II. La densidad de potencia absorbida se calcula mediante el trazado de rayos RAYS, teniendo en cuenta la estructura real del haz de microondas, cuya anchura no es despreciable frente al tamaño del plasma.

CLASIFICACION DOE Y DESCRIPTORES: 700350. Magnetic Confinement. Electrón Cyclotron-Resonance. Non-Inductive Current Drive. Plasma Heating. Stellarators.

CIEMAT-693

Centro de Investigaciones Energéticas, Medioambientales y Tecnológicas
Instituto de Investigación Básica.- MADRID

"Corriente contícua por ondas electrón-ciclotrón en estellaratores".

CASTEJON, F.; ALEJALDRE, C.; COARASA, J.A. (1992) 38 pp., 17 figs., 23 refs.

En este trabajo proponemos un método para calcular la corriente inducida por las microondas, en el rango de la frecuencia ciclotrónica electrónica, lo bastante rápido para ser incluído en un trazado de rayos y de esta forma tener en cuenta la complicada geometría de los estellaratores.Los efectos de las partículas atrapadas son particularmente importante en este método de inducción de corrientes en estellaratores, por lo tanto son tenidos en cuenta mediante la modificación que introducen en la eficiencia de la inducción de corrientes.

Básicamente el método consiste en integrar en el espacio de momentos el producto de la eficiencia relativista, corregida con los efectos de las partículas atrapadas, por la densidad de potencia absorbida en el espacio de fases. Esta última se calcula para una distribución Maxwelliana, ya que se supone que estamos en un régimen aproximadamente lineal. La influencia de las impurezas y de tener plasmas de otras especies que no sean protones se considera calculando la eficiencia para $Z_{eff} \neq 1$.

Finalmente se ha realizado un análisis numérico particularizado al Heliac Flexible TJ-II. La densidad de potencia absorbida se calcula mediante el trazado de rayos RAYS, teniendo en cuenta la estructura real del haz de microondas, cuya anchura no es despreciable frente al tamaño del plasma.

CLASIFICACION DOE Y DESCRIPTORES: 700350. Magnetic Confinement. Electrón Cyclotron-Resonance. Non-Inductive Current Drive. Plasma Heating. Stellarators.

CIEMAT-693

Centro de Investigaciones Energéticas, Medioambientales y Tecnológicas
Instituto de Investigación Básica.- MADRID

"Current drive by electron cyclotron waves in stellarators".

CASTEJON, F.; ALEJALDRE, C.; COARASA, J.A. (1992) 38 pp., 17 figs., 23 refs.

In this paper we propose a method to estimate the induced current by Electron Cyclotron waves fast enough, from the numerical point of view, to be included in a ray-tracing code, and yet accounting for the complicated geometry of stellarators. Since trapped particle effects are particularly important in this Current Drive method and in stellarator magnetic configuration, they are considered by the modification they introduce in the current drive efficiency.

Basically, the method consists of integrating the Fisch and Boozer relativistic efficiency, corrected with the effect of trapped particles, times the absorbed power per momentum interval. This one is calculated for a Maxwellian distribution function, assuming a nearly linear regime. The influence of impurities and of species which are not protons is studied, calculating the efficiency for plasmas with $Z_{eff} \neq 1$.

Finally, a numerical analysis particularized to TJ-II stellarator is presented. The absorbed power density is calculated by the ray tracing code RAYS, taking into account the actual microwave beam structure.

DOE CLASSIFICATION AND DESCRIPTORS: 700350. Magnetic Confinement. Electrón Cyclotron-Resonance. Non-Inductive Current Drive. Plasma Heating. Stellarators.

CIEMAT-693

Centro de Investigaciones Energéticas, Medioambientales y Tecnológicas
Instituto de Investigación Básica.- MADRID

"Current drive by electron cyclotron waves in stellarators".

CASTEJON, F.; ALEJALDRE, C.; COARASA, J.A. (1992) 38 pp., 17 figs., 23 refs.

In this paper we propose a method to estimate the induced current by Electron Cyclotron waves fast enough, from the numerical point of view, to be included in a ray-tracing code, and yet accounting for the complicated geometry of stellarators. Since trapped particle effects are particularly important in this Current Drive method and in stellarator magnetic configuration, they are considered by the modification they introduce in the current drive efficiency.

Basically, the method consists of integrating the Fisch and Boozer relativistic efficiency, corrected with the effect of trapped particles, times the absorbed power per momentum interval. This one is calculated for a Maxwellian distribution function, assuming a nearly linear regime. The influence of impurities and of species which are not protons is studied, calculating the efficiency for plasmas with $Z_{eff} \neq 1$.

Finally, a numerical analysis particularized to TJ-II stellarator is presented. The absorbed power density is calculated by the ray tracing code RAYS, taking into account the actual microwave beam structure.

DOE CLASSIFICATION AND DESCRIPTORS: 700350. Magnetic Confinement. Electrón Cyclotron-Resonance. Non-Inductive Current Drive. Plasma Heating. Stellarators.

CIEMAT-693

Centro de Investigaciones Energéticas, Medioambientales y Tecnológicas.
Instituto de Investigación Básica.- MADRID.

"Current drive by electron cyclotron waves in stellarators".

CASTEJON, F.; ALEJALDRE, C.; COARASA, J.A. (1992) 38 pp., 17 figs., 23 refs.

In this paper we propose a method to estimate the induced current by Electron Cyclotron waves fast enough, from the numerical point of view, to be included in a ray-tracing code, and yet accounting for the complicated geometry of stellarators. Since trapped particle effects are particularly important in this Current Drive method and in stellarator magnetic configuration, they are considered by the modification they introduce in the current drive efficiency.

Basically, the method consists of integrating the Fisch and Boozer relativistic efficiency, corrected with the effect of trapped particles, times the absorbed power per momentum interval. This one is calculated for a Maxwellian distribution function, assuming a nearly linear regime. The influence of impurities and of species which are not protons is studied, calculating the efficiency for plasmas with $Z_{eff} \neq 1$.

Finally, a numerical analysis particularized to TJ-II stellarator is presented. The absorbed power density is calculated by the ray tracing code RAYS, taking into account the actual microwave beam structure.

DOE CLASSIFICATION AND DESCRIPTORS: 700350. Magnetic Confinement. Electrón Cyclotron-Resonance. Non-Inductive Current Drive. Plasma Heating. Stellarators.